A Benzylideneacetophenone Derivative Induces Apoptosis of Radiation-Resistant Human Breast Cancer Cells via Oxidative Stress

Jeong Eon Park[1], Mei Jing Piao[1], Kyoung Ah Kang[1], Kristina Shilnikova[1], Yu Jae Hyun[1], Sei Kwan Oh[2], Yong Joo Jeong[3], Sungwook Chae[4] and Jin Won Hyun[1],*

[1]School of Medicine and Institute for Nuclear Science and Technology, Jeju National University, Jeju 63243,
[2]Department of Neuroscience, College of Medicine, Ewha Womans University, Seoul 03760,
[3]Department of Bio and Nanochemistry, Kookmin University, Seoul 02707,
[4]Aging Research Center, Korea Institute of Oriental Medicine, Daejeon 34054, Republic of Korea

Abstract

Benzylideneacetophenone derivative (1E)-1-(4-hydroxy-3-methoxyphenyl) hept-1-en-3-one (JC3) elicited cytotoxic effects on MDA-MB 231 human breast cancer cells-radiation resistant cells (MDA-MB 231-RR), in a dose-dependent manner, with an IC_{50} value of 6 μM JC3. JC3-mediated apoptosis was confirmed by increase in sub-G1 cell population. JC3 disrupted the mitochondrial membrane potential, and reduced expression of anti-apoptotic B cell lymphoma-2 protein, whereas it increased expression of pro-apoptotic Bcl-2-associated X protein, leading to the cleavage of caspase-9, caspase-3 and poly (ADP-ribose) polymerase. In addition, JC3 activated mitogen-activated protein kinases, and specific inhibitors of these kinases abrogated the JC3-induced increase in apoptotic bodies. JC3 increased the level of intracellular reactive oxygen species and enhanced oxidative macromolecular damage via lipid peroxidation, protein carbonylation, and DNA strand breakage. Considering these findings, JC3 is an effective therapy against radiation-resistant human breast cancer cells.

Key Words: Apoptosis, Benzylideneacetophenone derivative, Radiation resistance, Reactive oxygen species

INTRODUCTION

Breast cancer is one of the leading causes of cancer-mediated death among women in the world (Anderson and Jakesz, 2008). Changes in the lifestyles of women have a significant impact on the growing incidence rate of breast cancer (Takagi *et al*., 2015). Radiation therapy is an important part of conditioning regimens for breast cancer treatment. Radiotherapy significantly increases viability and post-operative local control in early-stage breast cancer patients (Jagsi, 2013). However, radiotherapy fails to control cancer growth in some breast cancer patients due to radiation resistance (Langlands *et al*., 2013). Thus, it is vital to research more efficient and reliable therapies to alleviate the risk of breast cancer.

Reactive oxygen species (ROS) are routinely formed as by-products of the breakdown of oxygen and play a crucial role in normal biological functions and abnormal pathological processes (Zhang *et al*., 2015). Cancer cells are characterized by elevated levels of intracellular ROS, which lead to abnormal metabolism, carcinogenesis stimulation, and mitochondrial malfunction (Kim *et al*., 2016). This suggests that induction of apoptosis in cancer cells via enhancing ROS to disturb antioxidant defense is a novel strategy for cancer therapy (Li *et al*., 2012). Apoptosis can occur via the death receptor pathway or the mitochondrial pathway (Huang *et al*., 2015; Tran *et al*., 2016). In the mitochondria-mediated intrinsic pathway, cell death signals are regulated by Bcl-2 family members, including the anti-apoptotic proteins B cell lymphoma-2 (Bcl-2) and the pro-apoptotic protein Bcl-2-associated X (Bax) (Reuter *et al*., 2008). ROS, which are mainly generated in mitochondria as byproducts of various metabolic processes, also regulate apoptotic signal transduction and mitochondrial membrane depolarization, causing continuous release of pro-apoptotic molecules into the cytosol (Jin *et al*., 2014). Mitogen-activated

www.biomolther.org

protein kinases (MAPKs), a family of stress-activated proteins comprising p38 MAPK, extracellular signal-regulated protein kinase (ERK), and c-Jun-N-terminal kinase (JNK), are activated by various extracellular stimuli. MAPKs regulate a series of physiological processes, including cell growth, differentiation, and apoptosis (Ahmed-Choudhury *et al.*, 2006). Accumulated data indicate that anticancer compounds regulate the functions of MAPK family members in many cancers. The benzylideneacetophenone derivative (1E)-1-(4-hydroxy-3-methoxyphenyl) hept-1-en-3-one (JC3) was discovered to be a neuroprotective agent against oxygen-glucose deprivation- and hydrogen peroxide-provoked cytotoxicity in cultured cortical cells (Jung *et al.*, 2008). In addition, JC3 potently activates intracellular signaling cascades including the Janus tyrosine (Jang *et al.*, 2009).

Understanding molecular pathways of anticancer drug is important for development of radio-sensitizers which is based on the cancer response to minimizing normal cell death, reduction of radiation dose, and resistance to radiotherapy or chemotherapy, etc. Radiation response modifier is designed for enhancing apoptosis of cancer cells while having much less effect on normal tissues. To develop modifier, *in vitro* studies are first step for novel radio-sensitizing agents driving cell death based on biological behavior of cancer cells (Alcorn *et al.*, 2013; Cho *et al.*, 2015; Taghizadeh *et al.*, 2015). In this study, JC3 was evaluated for whether it could be applied to modify radio-resistant breast cancer cells. Herein, we show that JC3 enhances apoptosis in MDA-MB 231 human breast cancer cells-radiation resistant cells (MDA-MB 231-RR) via mitochondrial apoptosis pathway regulation, ROS generation, and MAPK activation.

MATERIALS AND METHODS

Reagents

(1E)-1-(4-hydroxy-3-methoxyphenyl)hept-1-en-3-one (JC3) and JC3-dimer (Fig. 1A) were provided by professor Sei Kwan Oh (Ewha Womans University, Seoul, Korea) and dissolved in dimethylsulfoxide (DMSO). The final concentration of DMSO did not exceed 0.02% when JC3 was added to cells. 3-(4,5-Dimethylthiazol-2-yl)-2,5-diphenyltetrazolium bromide (MTT), propidium iodide (PI), Hoechst 33342, N-acetyl-L-cysteine (NAC), 1,3-bis(diphenylphosphino) propane (DPPP), 2',7'-dichlorodihydrofluorescein diacetate (DCF-DA), and actin antibody were purchased from Sigma-Aldrich Corporation (St. Louis, MO, USA). 5,5',6,6'-Tetrachloro-1,1',3,3'-tetraethyl-benzimidazolyl-carbocyanine chloride (JC-1) was purchased from Molecular Probes (Eugene, OR, USA). Bcl-2 and Bax antibodies were purchased from Santa Cruz Biotechnology Inc (Dallas, TX, USA). Caspase-3, caspase-9, JNK, phospho-JNK, p38 MAPK, phospho-p38 MAPK, ERK, phospho-ERK, and poly(ADP-ribose) polymerase (PARP) antibodies were purchased from Cell Signaling Technology (Beverly, MA, USA). SP600125, SB203580, and U0126 were purchased from Calbiochem (San Diego, CA, USA).

Cell culture

MDA-MB 231-RR were maintained at 37°C in an incubator with a humidified atmosphere of 5% CO_2 and cultured in RPMI 1640 medium containing 10% heat-inactivated fetal calf serum, streptomycin (100 μg/mL), and penicillin (100 units/mL).
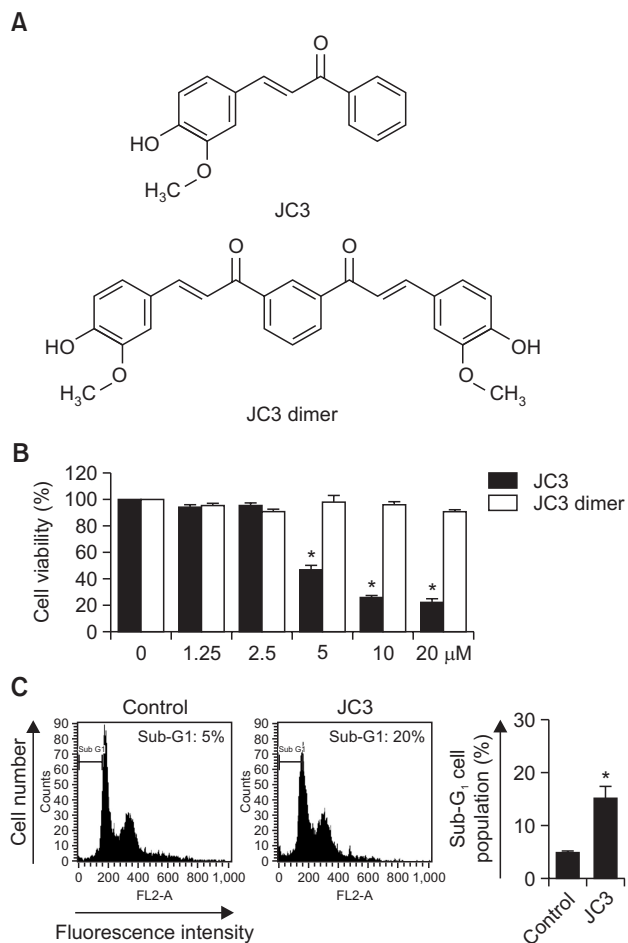

Fig. 1. Cytotoxic effects of benzylideneacetophenone derivatives on radiation resistant human breast cancer cells. (A) Structures of benzylideneace-tophenone derivatives (JC3 and JC3-dimer) are shown. (B) Cells were treated with the indicated concentrations (0, 1.25, 2.5, 5, 10, and 20 μM) of JC3 and JC3 dimer for 48 h. Cell viability was assessed using the MTT assay to determine the IC_{50} value. (C) The sub-G1 cell population was monitored by flow cytometry after PI staining. *Significant different from control cells ($p<0.05$).

Cell viability assay

Cells were treated with JC3 and JC3 dimer (1.25, 2.5, 5, 10, and 20 μM) at 37°C for 48 h. Thereafter, MTT was added to each well to obtain a total reaction volume of 200 μL. After incubation for 4 h at 37°C, the supernatant was removed by aspiration. The MTT solution was removed, and formazan crystals were solubilized in DMSO. The plates were shaken for 20 min at room temperature, and absorbance was measured at 560 nm (Maria *et al.*, 2016).

Detection of sub-G1 hypodiploid cells

Cells were seeded in a 6-well plate at a density of 2×10^5 cells/mL. Cells were treated with JC3 for 48 h, harvested, washed with phosphate-buffered saline (PBS), and fixed in 70% ethanol for 30 min at 4°C. Subsequently, the cells were incubated in the dark for 30 min at 37°C with a solution containing 100 μg/mL PI and 100 μg/mL RNase A. Cells were then examined in a FACSCalibur flow cytometer (Becton Dickinson,

East Rutherford, NJ, USA). Apoptotic cells were calculated as cells in the area corresponding to sub-G1 phase relative to total cells (Hao *et al*., 2015).

Detection of the mitochondrial membrane potential

Cells were seeded in a 6-well plate at a density of 1×10^5 cells/mL. After 24 h of plating, the cells were treated with 6 μM JC3 and incubated for an additional 48 h at 37°C. The mitochondrial membrane potential was analyzed using JC-1, a lipophilic cationic fluorescent dye that enters mitochondria and fluorescence changes from green to red as membrane potential increases. The mitochondrial membrane potential was analyzed by flow cytometry (Becton Dickinson). For image analysis, cells were stained with JC-1 (10 μg/mL) and affixed to microscope slides in mounting medium. Microscopy images were collected using a confocal microscope and the Laser Scanning Microscope 5 PASCAL program (Carl Zeiss, Oberkochen, Germany).

Western blot analysis

Cells were seeded in a 60 mm dish at a density of 2×10^5 cells/mL. Cells were harvested, washed twice with PBS, lysed on ice for 30 min in 120 μL of protein extraction solution and centrifuged at 10,000×g for 15 min. The supernatants were collected and the protein concentrations were determined using the Bio-Rad protein assay reagent kit (Bio-Rad, Hercules, CA, USA). Aliquots of the lysates (40 μg of protein) were boiled for 5 min and electrophoresed in 10% sodium dodecyl sulfate-polyacrylamide gel. The proteins were then transferred to nitrocellulose membranes, which were subsequently incubated with primary antibodies followed by a horseradish peroxidase-conjugated secondary antibody (Pierce, Rockford, IL, USA). Protein bands were detected using an enhanced chemiluminescence western blotting detection kit (Amersham, Little Chalfont, Buckinghamshire, UK), followed by exposure of the membranes to X-ray film.

Nuclear staining with Hoechst 33342

Cells were seeded in a 24 well plate at a density of 2×10^5 cells/mL. After 24 h of plating, the cells were treated with 6 μM JC3 and incubated for an additional 48 h at 37°C. After 48 h, cells were incubated with the DNA-specific fluorescent dye Hoechst 33342 (1.5 μL, 10 mg/mL) for 10 min at 37°C and visualized using a fluorescence microscope equipped with a Cool SNAP-Pro color digital camera (Media Cybernetics, Silver Spring, MD, USA).

Intracellular ROS detection

To detect ROS in JC3-treated cells, cells were seeded in 96-well plates at a density of 1×10^5 cells/mL. After 24 h, cells were treated with 6 μM JC3. After incubation for 48 h at 37°C, cells were incubated with DCF-DA (25 μM) for 30 min and then 2',7'-dichlorofluorescein fluorescence was detected and quantitated using a LS-5B spectrofluorometer (PerkinElmer, Waltham, MA, USA). DCF-DA fluorescence was detected (excitation, 485 nm; emission, 535 nm) using a FACSCalibur flow cytometer (Becton Dickinson), and images were collected using a confocal microscope.

Detection of DNA fragmentation

DNA fragmentation was examined and quantified using a cytoplasmic histone-associated DNA fragmentation kit (Roche Diagnostics, Mannheim, Germany) according to the manufacturer's instructions.

Lipid peroxidation assay

Lipid peroxidation was assessed using DPPP as a probe (Monica *et al*., 2010). DPPP reacts with lipid hydroperoxides to generate a fluorescent product, DPPP oxide, thereby providing an indication of membrane damage. Cells were treated with 6 μM JC3 for 48 h and then incubated with 20 μM DPPP for 30 min in the dark. Images of DPPP fluorescence were captured on a Zeiss Axiovert 200 inverted microscope at an excitation wavelength of 351 nm and an emission wavelength of 380 nm. Images were collected using a confocal microscope. Commercial enzyme immunoassay (Cayman Chemical, Ann Arbor, MI, USA) was employed to detect 8-isoprostane. Cells were treated with NAC for 1 h and then treated with JC3 at 37°C for another 48 h. A commercial enzyme-linked immunosorbent assay (ELISA) (Cayman Chemical) was used to detect 8-isoprostane according to the manufacturer's instructions.

Protein carbonyl formation

Cells were treated with 6 μM JC3 for 48 h at 37°C. The extent of protein carbonyl formation was determined using an Oxiselect™ protein carbonyl ELISA kit (Cell Biolabs, San Diego, CA, USA).

Single-cell gel electrophoresis (comet assay)

The degree of oxidative DNA damage was assessed by the comet assay (Singh, 2000). A cell suspension was mixed with 70 μL of 1% low-melting agarose (LMA) at 37°C, and the mixture was spread onto a fully frosted microscopic slide precoated with 200 μL of 1% normal melting agarose (NMA). After solidification of the agarose, the slide was covered with another 170 μL of 0.5% LMA, and then immersed in lysis solution (2.5 M NaCl, 100 mM Na-EDTA, 10 mM Tris, 1% Triton X-100, and 10% DMSO, pH 10) for 1 h at 4°C. The slides were subsequently placed in a gel electrophoresis apparatus containing 300 mM NaOH and 10 mM Na-EDTA (pH 10) and incubated for 30 min to allow for DNA unwinding and the expression of alkali-labile damage. An electrical field (300 mA, 25 V) was then applied for 30 min at 25°C to draw the negatively charged DNA towards the anode. The slides were washed three times for 10 min at 25°C in neutralizing buffer (0.4 M Tris, pH 7.5), and then washed once for 10 min at 25°C in 100% ethanol. Then, the slides were stained with 80 μL of 10 μg/mL ethidium bromide and observed using a fluorescence microscope and image analyzer (Komet 5.5, Kinetic Imaging Ltd., Wirral, UK). Tail length and percentage of total fluorescence in the comet tails were recorded for 50 cells per slide.

Statistical analysis

Values are expressed as the mean ± standard error of the mean. Results were analyzed using an analysis of variance and Tukey's test to determine pairwise differences. A *p*-value < 0.05 was considered significant.

RESULTS

Apoptotic cell death of JC3 on radiation resistant human breast cancer cells

MDA-MB 231-RR cells were treated with 0-20 μM JC3 and
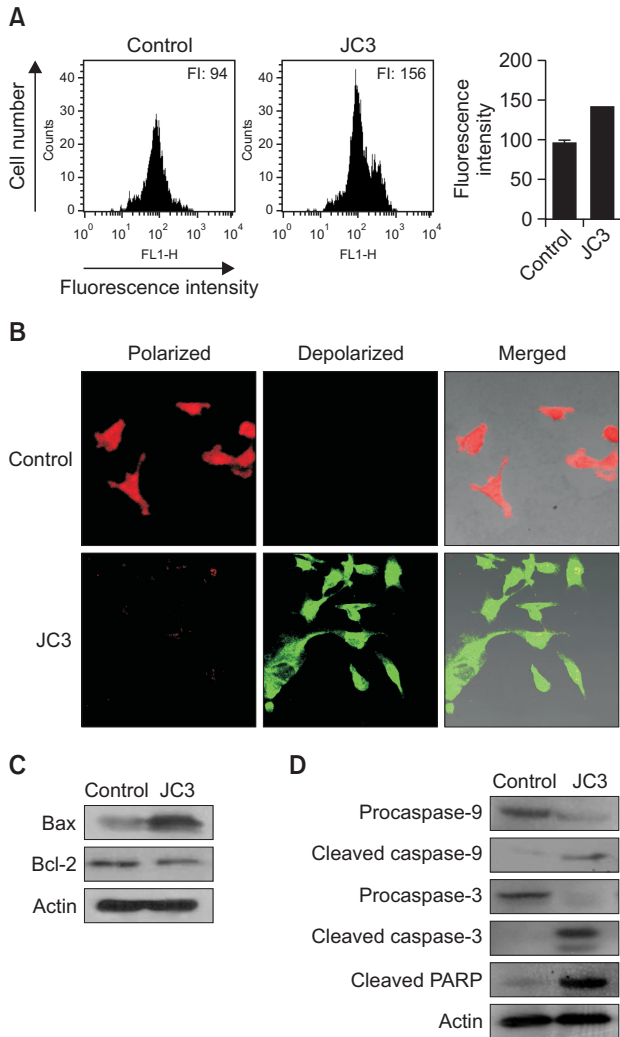
A

B

C

D

Fig. 2. Mitochondria-mediated apoptotic cell death of JC3 on radiation resistant human breast cancer cells. Mitochondria depolarization was measured by (A) flow cytometry and (B) confocal microscopy by staining with JC-1. *Significantly different from control cells ($p<0.05$). Expression levels of (C) Bax and Bcl-2 and (D) caspase-9, caspase-3, and PARP were monitored by western blot analysis.

A

B

Fig. 3. The MAPK-mediated apoptotic cell death of JC3 on radiation resistant human breast cancer cells. (A) Expression levels of phospho-ERK, phospho-JNK, and phospho-p38 were monitored by western blot analysis. (B) After treatment with MAPK inhibitors (U0126, SP600125, SB203580) and JC3, apoptosis was assessed by staining with Hoechst 33342. Arrows indicate apoptotic bodies. *Significantly different from control cells ($p<0.05$); #significantly different from JC3-treated cells ($p<0.05$).

JC3 dimer, and the IC$_{50}$ value was determined. Cytotoxicity was not observed upon treatment with the JC3 dimer at concentrations up to 20 μM; however, the IC$_{50}$ value of JC3 in MDA-MB 231-RR cells was 6 μM (Fig. 1B). To assess apoptosis, the sub-G1 population of JC3-treated cells was analyzed using a flow cytometer after staining with PI. The sub-G1 population of JC3-treated cells was remarkably larger than that of control cells (Fig. 1C).

Mitochondria-mediated apoptosis of JC3 on radiation resistant human breast cancer cells

JC3 triggered loss of mitochondrial membrane potential, as assessed by flow cytometric analysis (Fig. 2A). Furthermore, confocal microscopy analysis demonstrated that mitochondria of control cells exhibited strong red JC-1 fluorescence, indicative of mitochondrial membrane potential polarization, where-
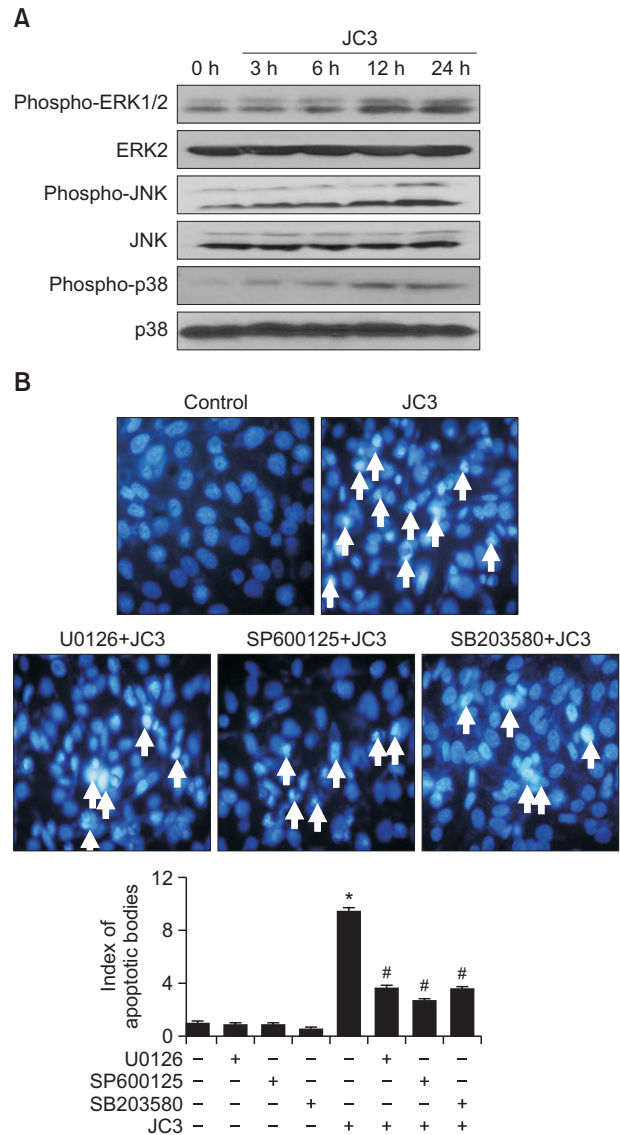
as JC3-treated cells exhibited an increased level of green fluorescence, indicative of mitochondrial membrane potential depolarization (Fig. 2B). Bcl-2 and Bax control mitochondrial apoptosis. JC3 decreased expression of the anti-apoptotic protein Bcl-2 and increased expression of the pro-apoptotic protein Bax (Fig. 2C). Caspase proteins, which are associated with the family of cysteine proteases, are necessary for apoptosis. Thus, caspase-9 and caspase-3 protein expression was investigated by western blot analysis. JC3-treated cells exhibited increased levels of the active (cleaved) forms of caspase-9 and caspase-3, resulting in increase of cleaved PARP (Fig. 2D).
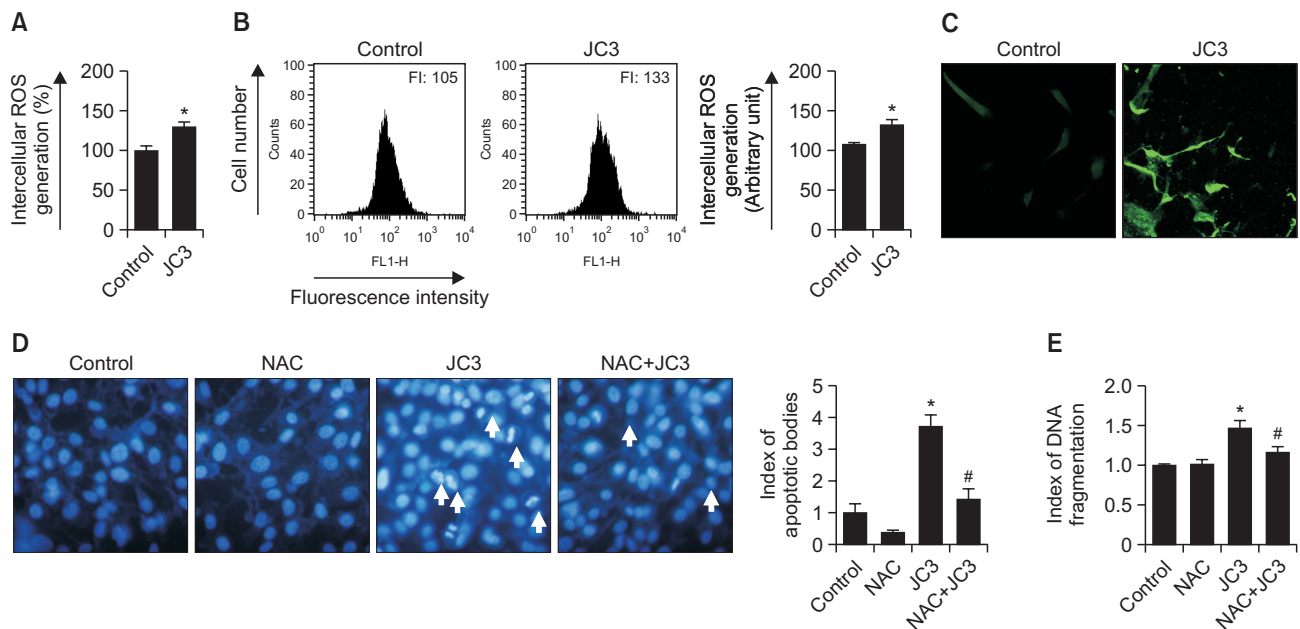
Fig. 4. Apoptotic cell death of JC3 via oxidative stress. ROS were measured as monitered by (A) spectrofluorometer, (B) flow cytometry and (C) confocal microscopy after staining with DCF-DA. (D) Apoptotic body formation (arrows) was assessed by fluorescence microscopy after Hoechst 33342 staining. (E) DNA fragmentation was assessed using a cellular DNA fragmentation kit. *Significantly different from control cells ($p<0.05$); #significantly different from JC3-treated cells ($p<0.05$).

Involvement of MAPK pathway of JC3-triggered apoptosis on radiation resistant human breast cancer cells

JC3 induced activation of ERK, JNK, and p38 MAPK in a time-dependent manner (Fig. 3A). Interestingly, U0126 (an inhibitor of ERK), SP600125 (an inhibitor of JNK) and SB203580 (an inhibitor of p38 MAPK) reduced the apoptotic cell death of JC3 (Fig. 3B).

JC3 induces generation of intracellular ROS in radiation resistant human breast cancer cells

JC3-treated MDA-MB 231-RR cells exhibited increased intracellular ROS generation, as assessed using a spectrofluorometer after staining with DCF-DA (Fig. 4A). Furthermore, flow cytometric data and confocal microscopy images indicated that the level of intracellular ROS was higher in JC3-treated cells than in control cells (Fig. 4B, 4C). To check whether JC3 induced apoptosis via oxidative stress, we assessed apoptosis following treatment with NAC, an antioxidant. Apoptotic body formation was higher in JC3-treated cells than in control cells, and NAC treatment reduced apoptotic body formation and DNA fragmentation induced by JC3 (Fig. 4D, 4E).

JC3 induces macromolecular cell damage via oxidative stress

Lipid peroxidation can be investigated by assessing the amount of 8-isoprostane released into the conditioned medium of cultured cells. DPPP reacts with lipid hydroperoxides to generate the highly fluorescent product DPPP oxide (DPPP=O) (Okimoto *et al.*, 2000). The fluorescence intensity in JC3-treated cells was significantly higher than that in control cells and was reduced by NAC treatment (Fig. 5A). Furthermore, the concentration of 8-isoprostane was notably increased in the JC3-treated group, but decreased in the

JC3 plus NAC-treated group (Fig. 5B). Protein carbonylation is a biomarker of oxidative stress-triggered protein damage (Dalle-Donne *et al.*, 2003). Consistent with the 8-isoprostane data, the protein carbonylation level was notably increased in JC3-treated cells; however, NAC remarkably prevented JC3-triggered protein carbonyl formation (Fig. 5C). DNA breaks induced by JC3 treatment were observed by the comet assay. DNA damage was notable in JC3-treated cells; however, NAC remarkably prevented JC3-triggered DNA damage (Fig. 5D).

DISCUSSION

Cell death is independently or coordinately regulated by multiple cellular and molecular mechanisms (Eisenberg-Lerner *et al.*, 2009). Apoptosis (a programmed cell death) is a genetically regulated form of cell death that is critical for many biological events and is an ultimate determinant of cancer cell fate (Eisenberg-Lerner *et al.*, 2009). Therapeutic approaches designed to destroy malignant cells via apoptosis are essential for the treatment of numerous forms of cancer (Laubenbacher *et al.*, 2009). Apoptotic cells display distinct morphological characteristics, cell shrinkage, dynamic membrane blebbing, chromatin condensation, and nuclear fragmentation. Apoptosis is associated with many pathways and signaling proteins, for example, death receptor family proteins, the nuclear transcription factor p53, and Bcl-2 family proteins (Ouyang *et al.*, 2012). Apoptosis occurs via the extrinsic (or death receptor) pathway, which is initiated from outside the cell through pro-apoptotic receptors on the cell surface, or the intrinsic (or mitochondrial) pathway, which is initiated within the cell (Laubenbacher *et al.*, 2009; Ouyang *et al.*, 2012).

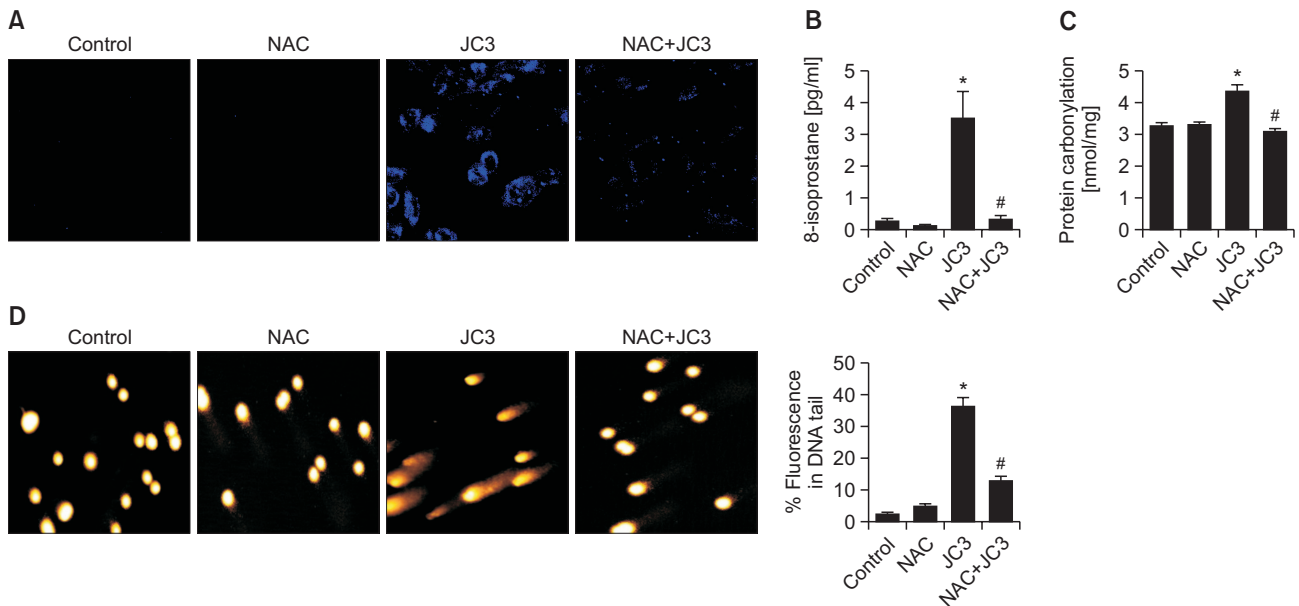Apoptotic signal disrupts mitochondrial inner membrane

Fig. 5. Cellular macromolecular damages by JC3-induced oxidative stress. Cellular lipid peroxidation was investigated by (A) confocal microscopy after staining with DPPP and (B) measuring 8-isoprostane levels. (C) Levels of protein carbonyl formation were assessed by a protein carbonylation assay. (D) DNA damage was monitored by the comet assay. *Significantly different from control cells ($p<0.05$); #significantly different from JC3-treated cells ($p<0.05$).

permeability, and consequently cytochrome c, which is a key electron carrier in the mitochondrial electron transport chain, is released into the cytosol. Leakage of cytochrome c sustains activation and hepta-oligomerization of the adaptor molecule apoptosis protease-activating factor, which induces formation of the apoptosome complex. This in turn induces cleavage of caspase-9 to initiate a caspase cascade, which activates other downstream caspases, resulting in apoptosis. Release of cytochrome c from mitochondria into the cytosol is controlled by the pro-apoptotic protein Bax and the anti-apoptotic protein Bcl-2 (Garrido *et al*., 2006). Bax is up-regulated, Bcl-2 is down-regulated, formation of apoptotic bodies is altered, and the caspase cascade is activated during apoptosis. In the present study, Bcl-2 was down-regulated concomitant with up-regulation of Bax upon JC3 treatment, leading to the loss of mitochondrial transmembrane potential, and activation of caspase-9 and caspase-3 (Fig. 2). Much evidence shows that anticancer agents can control the activities of MAPK family members in most carcinoma cells. Therefore, the induction of apoptosis by JC3 via activation of MAPKs was investigated in radiation resistant human breast cancer cells. ERK, JNK, and p38 were activated upon JC3 treatment, as evidenced by the increased levels of phosphorylated MAPKs and attenuation of JC3-induced apoptosis by these inhibitors (Fig. 3). It has reported that oxidative stress causes apoptosis (Li *et al*., 2014). In our study, oxidative stress induced by JC3 causes oxidative damage of DNA, lipids, proteins, leading to apoptosis of MDA-MB 231-RR breast cancer cells (Fig. 4, 5). Most of phenolic compound have potential for anti-cancer activity based on their chemical structures. The structure and activity relation between monomer and dimer is somewhat controversial. There is a report that JC3-dimer was more potent than monomer in the prostate cancer cells (Lee *et al*., 2016). To the best of our knowledge, JC3 might be working differently ac-

cording to different cells and detailed mechanism is remained for further study.

Taken together, JC3 may be a promising therapeutic candidate for the treatment of radiation-resistant human breast cancer cells via oxidative stress-mediated apoptosis.

REFERENCES

Ahmed-Choudhury, J., Williams, K. T., Young, L. S., Adams, D. H. and Afford, S. C. (2006) CD40 mediated human cholangiocyte apoptosis required JAK2 dependent activation of STAT3 in addition to activation of JNK1/2 and ERK1/2. *Cell. Signal.* **18**, 456-468.

Alcorn, S., Walker, A. J., Gandhi, N., Narang, A., Wild, A. T., Hales, R. K., Herman, J. M., Song, D. Y., Deweese, T. L., Antonarakis, E. S. and Tran, P. T. (2013) Molecularly targeted agents as radiosensitizers in cancer therapy-focus on prostate cancer. *Int. J. Mol. Sci.* **14**, 14800-14832.

Anderson, B. O. and Jakesz, R. (2008) Breast cancer issues in developing countries: an overview of the breast health global initiative. *World J. Surg.* **32**, 2578-2585.

Cho, H. J., Ahn, K. C., Choi, J. Y., Hwang, S. G., Kim, W. J., Um, H. D. and Park, J. K. (2015) Luteolin acts as a radiosensitizer in non-small cell lung cancer cells by enhancing apoptotic cell death through activation of a p38/ROS/caspase cascade. *Int. J. Oncol.* **46**, 1149-1158.

Dalle-Donne, I., Rossi, R., Giustarini, D., Milzani, A. and Colombo, R. (2003) Protein carbonyl groups as biomarkers of oxidative stress. *Clin. Chim. Acta* **329**, 23-38.

Eisenberg-Lerner, A., Bialik, S., Simon, H. U. and Kimchi, A. (2009)

Life and death partners: apoptosis, autophagy and the cross-talk between them. *Cell Death Differ.* **16**, 966-975.

Garrido, C., Galluzzi, L., Brunet, M., Puig, P. E., Didelot, C. and Kroemer, G. (2006) Mechanisms of cytochrome c release from mitochondria. *Cell Death Differ.* **13**, 1423-1433.

Hao, C., Deke, J., Fang, Q., Jianfeng, X., Long, Y. and Qianyi, X. (2015) HRP-3 protects the hepatoma cells from glucose deprivation-induced apoptosis. *Int. J. Clin. Exp. Pathol.* **8**, 14383-14391.

Huang, G., Mao, J., Ji, Z. and Ailati, A. (2015) Stachyose-induced apoptosis of Caco-2 cells via the caspase-dependent mitochondrial pathway. *Food Funct.* **6**, 765-771.

Jagsi, R. (2013) Progress and controversies: Radiation therapy for invasive breast cancer. *CA Cancer J. Clin.* **64**, 135-152.

Jang, S., Jung, J. C., Kim, D. H., Ryu, J. H., Lee, Y., Jung, M. and Oh, S. (2009) The neuroprotective effects of benzylideneacetophenone derivatives on excitotoxicity and inflammation via phosphorylated janus tyrosine kinase 2/phosphorylated signal transducer and activator of transcription 3 and mitogen-activated protein k pathways. *J. Pharmacol. Exp. Ther.* **328**, 435-447.

Jin, X., Song, L., Liu, X., Chen, M., Li, Z., Cheng, L. and Ren, H. (2014) Protective efficacy of vitamins C and E on p,p-DDT-induced cytotoxicity via the ROS-mediated mitochondrial pathway and NF-κB/FasL pathway. *PLoS ONE* **9**, e113257.

Jung, J. C., Jang, S., Lee, Y., Min, D., Lim, E., Jung, H., Oh, M., Oh, S. and Jung, M. (2008) Efficient synthesis and neuroprotective effect of substituted 1,3-diphenyl-2-propen-1-ones. *J. Med. Chem.* **51**, 4054-4058.

Kim, J., Kim, J. and Bae, J. S. (2016) ROS homeostasis and metabolism: a critical liaison for cancer therapy. *Exp. Mol. Med.* **48**, e269.

Laubenbacher, R., Hower, V., Jarrah, A., Torti, S. V., Shulaev, V. and Mendes, P. (2009) A systems biology view of cancer. *Biochim. Biophys. Acta* **1796**, 129-139.

Langlands, F. E., Horgan, K., Dodwell, D. D. and Smith, L. (2013) Breast cancer subtypes: response to radiotherapy and potential radiosensitisation. *Br. J. Radiol.* **86**, 20120601.

Lee, Y. H., Yun, J., Jung, J. C., Oh, S., and Jung, Y. S. (2016) Antitumor activity of benzylideneacetophenone derivatives via proteasomal inhibition in prostate cancer cells. *Pharmazie* **71**, 274-279.

Li, H., Horke, S. and Ulrich, F. (2014) Vascular oxidative stress, nitric oxide and atherosclerosis. *Atherosclerosis* **237**, 208-219.

Li, X., Xu, H., Dai, X., Zhu, Z., Liu, B. and Lu, X. (2012) Enhanced *in vitro* and *in vivo* therapeutic efficacy of codrug-loaded nanoparticles against liver cancer. *Int. J. Nanomedicine* **7**, 5183-5190.

Maria, K., Gemma, A. B., Giovanna, B., Paul, K. T. L. and Marie, G. (2016) Novel bisnaphthalimidopropyl (BNIPs) derivatives as anticancer compounds targeting DNA in human breast cancer cells. *Org. Biomol. Chem.* **14**, 9780-9789.

Monica, M., Andrea, C. and Luigi, A. (2010) Lipid oxidation in water-in-olive oil emulsions initiated by a lipophilic radical source. *J. Phys. Chem. B* **114**, 3550-3558.

Okimoto, Y., Watanabe, A., Niki, E., Yamashita, T. and Noguchi, N. (2000) A novel fluorescent probe diphenyl-1-pyrenylphosphine to follow lipid peroxidation in cell membranes. *FEBS Lett.* **474**, 137-140.

Ouyang, L., Shi, Z., Zhao, S., Wang, F. T., Zhou, T. T., Liu, B. and Bao, J. K. (2012) Programmed cell death pathways in cancer: a review of apoptosis, autophagy and programmed necrosis. *Cell Prolif.* **45**, 487-498.

Reuter, S., Eifes, S., Dicato, M., Bharat, B. A. and Diederich, M. (2008) Modulation of anti-apoptotic and survival pathways by curcumin as a strategy to induce apoptosis in cancer cells. *Biochemical Pharmacology* **76**, 1340-1351.

Singh, N. P. (2000) Microgels for estimation of DNA strand breaks, DNA protein crosslinks and apoptosis. *Mutat. Res.* **455**, 111-127.

Taghizadeh, B. Ghavami, L. Nikoofar, A. and Goliaei, B. (2015) Equol as a potent radiosensitizer in estrogen receptor-positive and -negative human breast cancer cell lines. *Breast Cancer* **22**, 382-390.

Takag, A., Kano, M. and Kaga, C. (2015) Possibility of breast cancer prevention: use of soy isoflavones and fermented soy beverage produced using probiotics. *Int. J. Mol. Sci.* **16**, 10907-10920.

Tran, Q., Lee, H., Park, J., Kim, S.H. and Park, J. (2016) Targeting cancer metabolism - revisiting the warburg effects. *Toxicol. Res.* **32**, 177-193.

Zhang, C., Cao, S., Toole, B. P. and Xu, Y. (2015) Cancer may be a pathway to cell survival under persistent hypoxia and elevated ROS: a model for solid-cancer initiation and early development. *Int. J. Cancer* **36**, 2001-2011.